

# Fluxes and sources of nutrients and trace metals atmospheric deposition in the northwestern Mediterranean

Karine Desboeufs<sup>1</sup>, Elisabeth Bon Nguyen<sup>1</sup>, Servanne Chevaillier<sup>1</sup>, Sylvain Triquet<sup>1</sup>, and François Dulac<sup>2</sup>.

1. Laboratoire Interuniversitaire des Systèmes Atmosphériques (LISA), IPSL, UMR CNRS 7583, Université Paris-Est Créteil et Université Paris-Diderot, Créteil, France
2. Laboratoire des Sciences du Climat et de l'Environnement (LSCE), UMR 8212 CEA-CNRS-UVSQ, IPSL, Université Paris-Saclay, CEA Saclay 701, Gif-sur-Yvette, France

## Abstract

Total atmospheric deposition was collected on a weekly basis over 3.5-yr (March 2008-October 2011) at a remote coastal site on the west coast of Corsica Island. Deposition time series of macro and micro-nutrient (N, P, Si, Fe), and trace metals (As, Cr, Cu, Mn, Ni, V, Zn) are investigated in terms of variability and source apportionment (from fluxes of proxies for aerosol sources (Al, Ti, Ca, Na, Mg, S, Sr, K, Pb)). The highest fluxes are recorded for Si, P, then Fe for nutrients, and for Zn and Mn for trace metals. For the majority of elements, data show some weeks with high episodic fluxes, except for N, Cr and V which present the lowest variability. Twelve intense mineral dust deposition events are identified during the sampling period. The contribution of these events to the fluxes of Fe and Si represents 52% and 57% of their total fluxes, respectively, confirming the important role of these sporadic dust events on the inputs of these elements in the Mediterranean. For N and P, the contribution of these intense dust deposition events is lower and reaches 10 and 15%, respectively. Out of these most intense events, positive matrix factorization (PMF) was applied to our total deposition database in order to identify the main sources of nutrients and trace metals deposited. Results show that P deposition is mainly associated to anthropogenic biomass burning inputs. For N deposition, inputs associated to marine sources (maybe associated to the reaction of anthropogenic N on NaCl particles) and anthropogenic sources are quasi-similar. A good correlation is obtained between N and S fluxes, supporting a common origin associated to the inorganic secondary aerosol, i.e. ammonium sulfate. For trace metals, their origin is very variable: with a large contribution of natural dust sources for Ni or Mn and on the contrary of anthropogenic sources for V and Zn.

## 34 **1. Introduction**

35 The Mediterranean Sea is a semi-enclosed basin situated at the interface between contrasted  
36 continental areas of three continents, namely southern Europe, northern Africa and the  
37 Middle East, which coastal areas are heavily populated. Thus, the Mediterranean basin  
38 continuously receives anthropogenic aerosols from industrial and domestic activities from all  
39 around the basin and other parts of Europe (Sciare et al., 2008; Becagli et al., 2012). In addition  
40 to deposition from this anthropogenic background, seasonal inputs from biomass burning  
41 occur mainly during dry summers (Chester et al., 1996; Guieu et al., 1997), and strong  
42 deposition pulses of mineral dust from the Sahara are superimposed (Guerzoni et al. 1999a),  
43 with some 'extreme events' with dust deposition fluxes as high as  $22 \text{ g m}^{-2}$  as recorded in 2004  
44 (Bonnet and Guieu, 2006) on very short time scales of a few hours to a few days.

45 A number of key elements for marine biota are associated to those inputs. Thus, several  
46 authors showed that the atmospheric deposition of aerosols constitutes the main source of  
47 major nutrients, as N, P or Fe to the surface open waters of the Mediterranean Sea in the  
48 summer/autumn period when surface water stratification prevents inputs from deep water  
49 by vertical mixing (Guerzoni et al., 1999a; Bonnet and Guieu, 2006; Krom et al., 2010; Pulido-  
50 Villena et al., 2010; Richon et al., 2018a, Violaki et al., 2018). Besides the classical nutrients (N,  
51 P and Fe), the aerosols also carry trace metals (hereafter called TMs) such as Cr, Cu, Ni, Mn or  
52 Zn that are known to have a biological role, often as cofactors or part of cofactors in enzymes  
53 and as structural elements in proteins (Morel and Price, 2003). The recent study of Ridame et  
54 al. (2011) suggests that the trace metals released by Saharan dust could stimulate nitrogen  
55 fixation in summer in the Mediterranean Sea. This assumption is supported by the works of  
56 Tovar-Sanchez (2014) which show that the trace metals concentrations in surface microlayer  
57 of the Mediterranean Sea is correlated with the atmospheric deposition of mineral dust.  
58 However, it has been also suggested that the atmospheric deposition of particulate pollutants  
59 is responsible for the contamination of the Mediterranean waters in trace metals (Bethoux et  
60 al., 1990; Guerzoni et al., 1999b). Gallisai et al. (2014) also show negative effects of dust  
61 deposition on chlorophyll, coinciding with regions under a large influence of aerosols from  
62 European origin.

63 Thus, the partitioning/mixing between anthropogenic vs. natural atmospheric inputs is critical  
64 to estimate and predict the role of the atmospheric deposition on marine biosphere and

65 associated services (Richon et al., 2018b). However in the Mediterranean Sea, the existing  
66 database on atmospheric fluxes of nutrients and trace metals remain quite limited. Most  
67 studies are focused on total deposition of dust and/or macro-nutrients as P and N (e.g.  
68 Markaki et al., 2010). This approach do not include the variety of nutrients and do not enable  
69 to distinguish the origin of nutrient-bearing particles. Moreover, the studies on trace metals  
70 deposition (Cd, Pb...) often show an influence of local sources (Guieu et al., 2010), limiting the  
71 reliability of these data. At the difference of atmospheric deposition, the source  
72 apportionment of suspended particles over the Mediterranean, from PMF method, has been  
73 highly investigated in recent works and showed a large spatial variability in source  
74 contributions (Becagli et al., 2012 and 2017; Calzolari et al., 2015; Amato et al., 2016; Diapouli  
75 et al., 2017). The signature of continental pollution sources was observed even in remote area,  
76 as central Mediterranean islands (Calzolari et al., 2015). Yet, PM concentrations and sources  
77 are probably different of sources of deposited particles which depends on aerosols size  
78 distribution and precipitation patterns, among other factors. Thus, in a context of  
79 anthropogenic changes, it is crucial to distinguish between anthropogenic vs natural  
80 atmospheric inputs of nutrients in order to assess how the evolution of chemical atmospheric  
81 forcing will modify the marine nutrient cycling.

82 Here we show a 3.5-yr long continuous series of total deposition fluxes of macro and micro-  
83 nutrient (N, P, Si, Fe), trace metals (As, Cr, Cu, Mn, Ni, V, Zn) and source tracers (Al, Ti, Ca, Na,  
84 Mg, S, Sr, K, Pb) at a remote coastal site in Corsica. Between March 2008 and October 2011, a  
85 monitoring station has been operated with a weekly sampling time step for total bulk  
86 deposition. In order to assess the contribution of sources in the fluxes of nutrients, a work on  
87 the source apportionment of various nutrients and TMs was carried out from these data (PMF  
88 method). A specific attention was also given on the different types of extreme atmospheric  
89 events which are relevant regarding the biogeochemistry in the Mediterranean Sea. They  
90 include Saharan events and intense summer storms that trigger the washout of the  
91 atmosphere over an altitude of several thousands of meters in a short time.

92  
93  
94

95        **2. Material and methods**

96        **2.1. Sampling site and protocol**

97 Total bulk deposition (i.e. dry + wet deposition) was sampled weekly from March 2008 to  
98 October 2011 using an open collector for nutrients and TMs analyses, except for N which the  
99 analyses started only from November 2009. Sampling was conducted at Cap Cuittone  
100 (42.44°N, 8.66°E, 190 m above sea level). The sampling site is on the Mediterranean coast of  
101 the National Corsica Park (Parc Naturel Régional de Corse) at 16 km to the SSE of Calvi, the  
102 main city in that part of the island which has no important industry (~5500 inhabitants), and  
103 about 3.5 km N of the village of Galeria (~350 inhabitants). Consequently, the data from this  
104 site could be considered representative of the open western Mediterranean Sea.

105 The sampler is a 120-mm diameter PTFE Teflon® funnel (collection aperture 0.0113 m<sup>2</sup>)  
106 machined on a circular base with a thread adapted to 500 mL polypropylene (PP) Nalgene®  
107 bottle neck. The funnel stem is a long tapered stem in such a way that it soaks in the preloaded  
108 acid for limiting the evaporation of collected water. All the deposition sampling materials  
109 (Teflon®-PTFE capped funnels, 500 mL and 60 mL Nalgene® PP bottles, and 60 mL PP boxes  
110 with a screwing cap for bottle's corks) were thoroughly washed with hydrochloric acid at the  
111 ultra-clean laboratory of LISA following a protocol adapted for ultra-clean sampling  
112 (Heimburger et al., 2012). Before deployment, the sampling bottles are preloaded with 50 mL  
113 of hydrochloric acid (2%v/v) and weighed. Each funnel coupled to its bottle preloaded was  
114 deployed on the site at 2 m height. The position was controlled by a spirit level to ensure that  
115 the funnel aperture was horizontally leveled. Each week, before collection, the internal  
116 surface of the funnel was rinsed with 60 mL of 2%v/v ultrapure hydrochloric acid in ultrapure  
117 water, taking care to flush all the surface. The rinsing solution was collected in the sample  
118 bottle to be removed and replaced by a new 500 mL PP bottle for the next week. The funnel  
119 was replaced by a new one every 6 months. Field blanks were performed at the funnel  
120 installation and removal, but also from time to time by repeating twice the sampling  
121 procedure. One permanent staff of the Corsica National Park was carefully advised and  
122 performed sampling during all the monitoring period.

123

124

## 125        **2.2.    Chemical analyses**

126        In the laboratory, total atmospheric deposition sampled bottles were weighted. The amount  
127        of rainwater collected in the funnel was deduced by subtracting added acid solution (i.e. 110  
128        mL) to the sample total mass found in the bottle. Each sample was shaken and then 15 mL  
129        were immediately transferred into a PE sampling vial to measure the size distribution of the  
130        particulate phase (not discussed here). The rest of the sample was filtered before analysis with  
131        acid washed Nuclepore® polycarbonate filters (0.2- $\mu$ m porosity). The filters were analysed by  
132        wavelength dispersive X-ray fluorescence (PW-2404 spectrometer by PANalytical™) for the  
133        particulate elemental concentrations for elements from Na to Pb, including macro (P) and  
134        micro-nutrient (Fe, Si), trace metals (As, Cr, Cu, Mn, Ni, V, Zn), and source tracers (Al, Ti, Ca,  
135        Na, Mg, S, Sr, K, Pb). Analyses of the filtered aqueous sample were performed by Inductively  
136        Coupled Plasma- Atomic Emission Spectrometry (ICP-AES, Spectro ARCOS Ametek®) coupled  
137        with a CETAC ultrasonic nebulizer for dissolved elemental concentrations of as many trace  
138        metals as possible (altogether 45 elements were analysed; Desboeufs et al., 2014). Due to the  
139        time between collection and analyses, the preservation of N speciation was not guaranteed  
140        and in consequence data are expressed as total N. The total dissolved inorganic N  
141        concentrations were obtained by adding  $\text{NH}_4^+$  concentrations and  $\text{NO}_3^-$  and  $\text{NO}_2^-$   
142        concentrations determined by ionic chromatography (Professional IC 850 by Metrohm®).  
143        Field blank concentrations are significantly inferior to sample concentrations for all the  
144        studied elements. They represent in average from  $1.4\% \pm 1.3\%$  (Mn) to  $12\% \pm 6\%$  (Fe) of  
145        studied elements concentrations, with a maximum contribution of 19% for trace metals (V)  
146        and 22% for major nutrients (Fe). Field blank concentrations are subtracted to samples  
147        concentrations collected in the same period.

148        The weekly elemental deposition fluxes were calculated from concentrations of all chemical  
149        species measured in dissolved and particulate samples by considering the sampler area and  
150        the total liquid volume (preloading + rinsing + rain). The total elemental deposition fluxes were  
151        estimated by adding particulate and dissolved fluxes except for N assumed totally acid-  
152        soluble. Atmospheric nitrogen exists in particulate phase but also as gaseous species ( $\text{NO}_x$ ,  
153         $\text{HNO}_3$ ,  $\text{NH}_3$ ). In our study, the used bulk collector has a design very close to the one of bulk  
154        collectors used during ADIOS project which are not optimized to collect gaseous nitrogen by  
155        dry deposition (Markaki et al., 2008). However, wet deposition including both washed-out

156 particulate and gaseous nitrogen, measured N fluxes in this study will be considered mainly  
157 representative of bulk deposition of aerosol particles plus wet deposition of gaseous N.

### 158 **2.3. Dry vs. wet deposition**

159 The speciation between wet and dry deposition is a critical parameter to estimate the  
160 potential dissolved fluxes of nutrients. Precipitation (mm) was estimated on the site from the  
161 amount of water in the sample. The precipitation occurrences are in agreement with the  
162 rainfall records on Calvi airport which is distant by about 15 km. Since they are more  
163 representative of local rainfall, precipitation estimated from our samples were used for the  
164 attribution of deposition fluxes to wet vs. dry deposition. Wet deposition was considered  
165 when rainfall was larger than 1 mm during the sampling period. The threshold value of 1 mm  
166 integrates the uncertainties on the weighing of samples in order to ascertain that the rainfall  
167 was real. Samples which present no precipitation or rainfall lower than 1 mm, are considered  
168 as dry deposition. In consequence, dry deposition is assimilated to wet deposition when  
169 happening the same week as a precipitation event. This method underestimates dry  
170 deposition, and provides a lower estimates of deposition dry event number vs total deposition  
171 event number.

### 172 **2.4. Positive Matrix Factorization (PMF)**

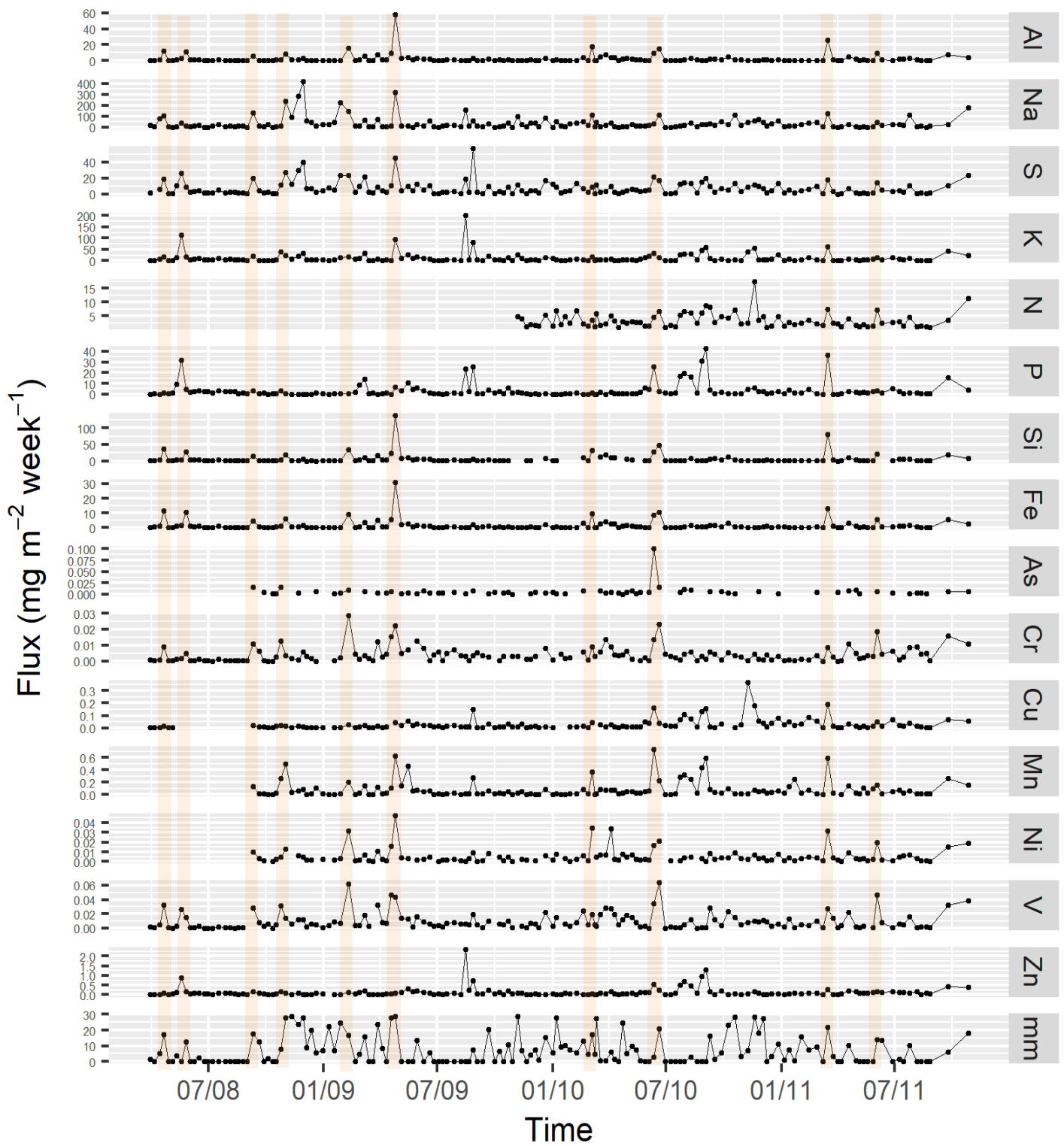
173 Multivariate statistical methods, such as factor analysis, are widely used to identify source  
174 signatures and explore source–receptor relationships using the trace element compositions  
175 of atmospheric aerosols (e.g., Polissar et al., 2001, Calzolari et al., 2015) and precipitation  
176 (Keeler et al., 2006; Gratz et al., 2013). Since many sources emit characteristic relative  
177 amounts of certain trace elements, source–receptor techniques can be used with an  
178 understanding of these elemental signatures to identify the major sources influencing a given  
179 receptor site.

180 We applied EPA PMF v5.0 (Norris et al., 2014) to the matrices of tracers, nutrient and TMs  
181 total deposition measurements. PMF is a multivariate statistical technique that uses weighted  
182 least-squares factor analysis to decouple the matrix of observed values (X) into two matrices  
183 representing the factor scores (G) and factor loadings (F), as represented by the equation  
184  $X = GF + E$ , where E is the residual matrix representing the difference between observed and  
185 predicted values (Paatero and Tapper, 1994; Paatero, 1997). Prior to applying PMF, we used

186 the weekly deposition fluxes and we replaced fluxes reported as less than median detection  
187 limit (MDL) with the median value. The uncertainties for each samples correspond to the sum  
188 of uncertainties in sample collection (i.e. 10%) and analytical measurement (standard  
189 deviation of three replicate analysis for each sample). We included all valid samples, excluding  
190 the samples that we identified as extreme outliers, i.e. samples corresponding to dust events  
191 and high As deposition (12 samples) (see section extreme events). The deposition fluxes for  
192 21 elements is used; i.e macro and micro-nutrient (N, P, Si, Fe) and TMs (As, Cr, Cu, Mn, Ni, V,  
193 Zn) and tracer elements (Al, Ti, Ca, Na, Mg, sea-salt S (S<sub>ss</sub>), Pb, K, and excess S (S<sub>exc</sub>). The  
194 estimation of S<sub>ss</sub> fluxes is obtained from Na fluxes on the basis of typical seawater S/Na ratio  
195 (Henderson and Henderson, 2009) and S<sub>exc</sub> fluxes in subtracting S<sub>ss</sub> to total S fluxes. Since S  
196 was used as sources tracers, the discrimination between ssS and excS enabled to have a best  
197 constrain on signature of sources. Elements with a signal-to-noise (S/N) ratio <5 were  
198 categorised as “weak” (i.e. As and N) and hence down-weighted so that the user-provided  
199 uncertainty was increased by a factor of three (Norris et al., 2014). The variability in the PMF  
200 solution was estimated using a block bootstrap technique, which calculates the stability of the  
201 model solution by randomly re-sampling blocks of the input dataset and computing the  
202 variability between model solutions. We applied 100 bootstrap runs to the PMF base run with  
203 the lowest Q value. We determined the final factor profiles based on our ability to identify all  
204 the factors, the robustness of Q values, the ability of the model to replicate measured results,  
205 and the bootstrap results.

### 206 **3. Results and discussion**

207 The 3.5-yr time-series of weekly fluxes (195 samples) for nutrients, TMs, major source tracer  
208 elements (Al, Na, S and K) and precipitation are presented in Figure 1. Corresponding time-  
209 series of other source tracer elements (Ti, Mg, Sr, Pb) are available in supplement with the  
210 total atmospheric fluxes data. The highest fluxes are recorded for Si, P then Fe for major  
211 nutrients and for Zn and Mn for trace metals. 51% of the samples, i.e. 99 samples, sustained  
212 at least one event of precipitation during the week of sampling and are here referenced as  
213 wet deposition. In our set of 195 samples, 21 presented a rainfall higher than 20 mm and the  
214 highest weekly rainfall recorded is 29 mm. However, no systematic link is observed between  
215 the biggest rain event and the nutrients or metals fluxes.



216  
 217 **Figure 1: Temporal variability of bulk weekly fluxes from March 2008 to October 2011 for main markers,**  
 218 **nutrients and trace metals, and rainfall on the same period. The 10 most intense dust event are displayed in**  
 219 **the boxes in orange (see details in “The case of high deposition events”)**  
 220



221 The results emphasize large differences in timing of deposition fluxes between the studied  
222 elements. But for all the elements, data display some weeks with high episodic fluxes. Due to  
223 the sporadic character of specific events such as dust storms or forest fires giving rise to high  
224 deposition events, it is known that the fluxes of elements associated to these sources are often  
225 important on a short period. For example, for elements such as aluminium associated with  
226 dust events, a half or more of the annual deposition flux may occur in one event of a few days  
227 or even hours (Guieu et al., 2010), and high deposition events ( $>1 \text{ g m}^{-2}$ ) are responsible for  
228 the inter-annual variability of the Al deposition flux in the western Mediterranean basin (Löye-  
229 Pilot and Martin, 1996). As a consequence, the fluxes linked to these extreme events can  
230 dominate and hide the influence of more continuous emission sources. In our dataset, this is  
231 the cases of Si, Fe and As, for which 25% of total fluxes on 3.5 years is delivered by 1 to 3  
232 weekly samples, whereas for the majority of nutrient and TMs, 25% of total fluxes are  
233 constituted from the 5 to 8 highest events. The most obvious case is for As which 23% of the  
234 total flux is obtained in only one week during June 2010 ( $0.1 \text{ mg m}^{-2} \text{ week}^{-1}$ ). This event  
235 corresponds to one event of wet deposition of 7 mm, i.e. no particularly intense rain, and is  
236 concomitant with high fluxes for the other studied elements.

### 237 **3.1. Seasonal variability**

238 Monthly total and wet fluxes have been estimated to investigate the seasonal variability of  
239 the measured elements inputs over the northwestern Mediterranean (Figure 2). A large  
240 variability in the monthly deposition fluxes of all the elements is observed in agreement with  
241 the episodic pattern of weekly inputs. Nutrients deposition presents a clear seasonal pattern:  
242 P with the major deposition fluxes in summer, and N in winter, whereas the main fluxes are  
243 observed in spring for Fe, Si, Cr, Ni and V. For As, excluding June, which shows its highest  
244 monthly mean flux due to the intense event of June 2010, the maximum of fluxes are recorded  
245 at the end of summer and beginning of autumn. For Mn, no clear seasonality is observed. A  
246 monthly flux predominates in August and November for Zn and Cu, respectively, reaching at  
247 least twice the other monthly fluxes. For all the elements, the wet deposition predominates  
248 the total fluxes between October and April in agreement with the highest rainfall recording  
249 during this period, whereas dry deposition is the main way of input in May, July and August.  
250 Our results are in agreement with the seasonal pattern observed in the 1980's for Si and Fe  
251 deposition at Capo Cavallo, 8 km more North on the Corsican coast (Bergametti et al., 1989).

252 The maximum of deposition during spring is explained by the concomitance of rainfall and  
253 high dust concentrations, whereas Si and Fe atmospheric aerosols concentrations present  
254 their maximum in summer during the dry season. This emphasizes that the below-cloud  
255 scavenging of aerosol is the predominant process explaining atmospheric deposition of dust-  
256 related elements in this period. For the elements mainly associated to dry deposition, i.e. Zn,  
257 P and Cr, Bergametti et al. (1989 and 1992) observed that the highest deposition was typically  
258 associated with the period of their highest aerosols concentrations in summer. This is not the  
259 case for Cr in our results, which follows the Si and Fe behavior. At the difference of our Corsica  
260 site, no clear seasonal variability is observed for the deposition fluxes recorded at Cap Ferrat,  
261 170 km more NNE on the French continental coast, a site affected by the anthropogenic  
262 influences from continental Europe (Pasqueron de Fommervault et al., 2015). That could be  
263 the case for Mn atmospheric fluxes on our site.

264 The case of N deposition is specific, since the N deposition flux corresponds mainly to total  
265 aerosol and wet gaseous deposition inputs in our samples. The general pattern for N with  
266 highest fluxes in winter could be linked to the thermal instability of the ammonium nitrate,  
267 which is the dominant form of N in aerosol particles associated to a decrease of rain events  
268 during the hot season, and to extremely typical intense nitrate episodes recorded from  
269 November to March in the western Mediterranean basin associated to maximum wet  
270 deposition (Querol et al., 2009). The highest N deposition flux is recorded in November 2010  
271 (Figure 1), this event is associated with wet deposition and is coincident with a deposition  
272 peak for Cu and K.

273

274

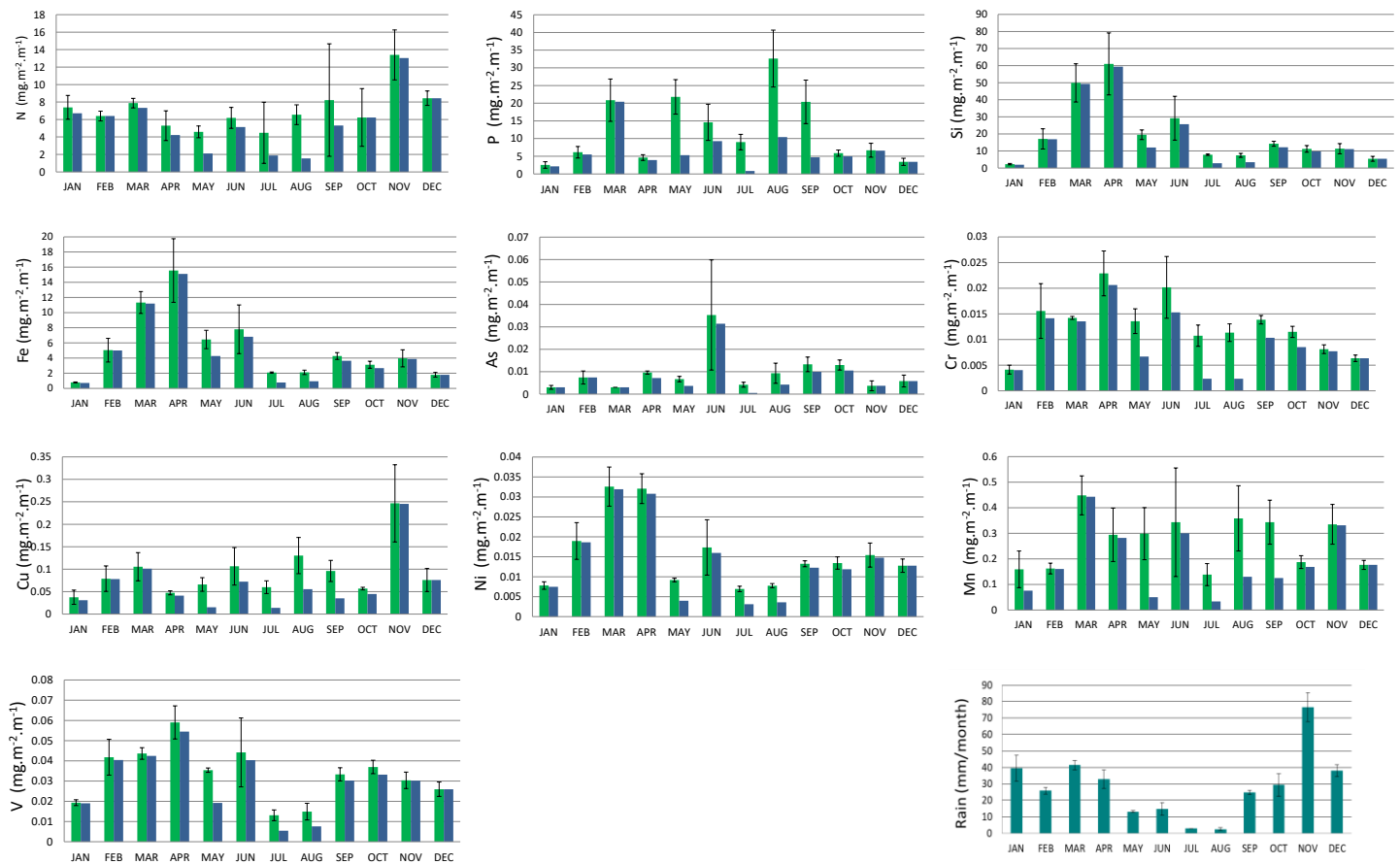
275

276

277

278

279



280 **Figure 2: Temporal variation of monthly total (green bars) and wet (blue bars) deposition and precipitation during the**  
 281 **sampling period March 2008–October 2011. Bars indicate standard deviations over the weekly values available over the**  
 282 **period.**

283

### 284 **3.2. Inter-annual variability**

285 The average annual total deposition fluxes for the major nutrients and trace metals during the  
 286 3.5 years of sampling are presented in Table 1. Among major nutrients, the most abundant  
 287 nutrients in bulk deposition is Si followed by P and N which have fluxes in the same order of  
 288 magnitude. The highest annual fluxes recorded for N in comparison to Fe is due to the sporadic  
 289 pattern of Fe fluxes in comparison to N that shows more regular weekly fluxes. For trace  
 290 metals, the highest annual fluxes are observed for Zn, Mn and Cu whereas the other trace  
 291 metals have fluxes smaller by one order of magnitude. Except for Ni, the standard deviations  
 292 on the mean fluxes are larger than 15%, and reach more than 50% for P, As and Cu, meaning  
 293 a large inter-annual variability of their deposition, in agreement with the high recorded  
 294 sporadic weekly fluxes for these elements. Our results are compared with other fluxes in  
 295 Corsica (Table 1) as reported in the literature. Data show that for trace metals, the recorded

296 values are in the same order of magnitude of previous measurements in Corsica. On the  
 297 contrary, for the major elements as Fe, Si and N except for P, our deposition flux values are  
 298 much lower than the previous ones obtained in Corsica (Table 1) and globally in the western  
 299 Mediterranean (Bonnet et al., 2006; Pasqueron de Fommervault et al., 2015). A net decrease  
 300 in N deposition is also observed between the 1990's and now in Europe (Waldner et al., 2014).  
 301 The only element with highest deposition fluxes in comparison to the literature is P, suggesting  
 302 an increase in atmospheric fluxes for this element. Keeping in mind that dry deposition events  
 303 can be underestimated by our method, the wet fluxes predominate the total deposition fluxes  
 304 ( $\geq 64\%$ ) for the majority of elements except for P and Zn, for which less than half of the total  
 305 flux is associated to precipitation. This is in agreement with the seasonality of deposition of  
 306 these elements which is high in summer when the contribution of dry deposition is the  
 307 highest.

308

309 **Table 1: Left part, annual total, wet and dry deposition fluxes ( $\text{mg m}^{-2} \text{y}^{-1}$ ) of major nutrients and trace elements, and**  
 310 **relative contribution (%) of wet periods on the total fluxes measured at Capo Cuittone, Corsica, between March 2008 and**  
 311 **October 2011. Right part, annual deposition fluxes at various sites in Corsica available in the literature.**

Ele- ment	Total Flux		Wet Flux	Dry Flux		Capo Cavallo <sup>a</sup>	Pirio <sup>b</sup>	Ostrioni <sup>c</sup>	Bavella <sup>d</sup>
	Average	Range	Average	Average	% wet	Fev. 1985 to Nov. 1987	Jan. 1995 to Mar. 1997	Jun. 2001 to May 2002	1984- 1986
<b>N</b>	143 $\pm$ 61	81-167	107.6	19.9	84%			355-377*	644-766
<b>P</b>	149 $\pm$ 79	114-253	73.3	75.4	49%	24.2-40.1		43.2	
<b>Fe</b>	67 $\pm$ 10	65-77	56.2	10.5	84%	395-406	118-156	1188	
<b>Si</b>	246 $\pm$ 61	197-280	206.7	39.3	84%				
<b>As</b>	0.14 $\pm$ 0.07	0.10-0.20	0.10	0.06	64%				
<b>Cr</b>	0.16 $\pm$ 0.04	0.12-0.19	0.11	0.05	69%				
<b>Cu</b>	1.06 $\pm$ 1.07	0.44-2.16	0.72	0.33	68%	2.3-3.7	0.7-1.4		
<b>Mn</b>	3.7 $\pm$ 1.4	2.5-5.2	2.15	1.20	64%	12.5-15.2	6.3-6.5		
<b>Ni</b>	0.21 $\pm$ 0.01	0.14-0.24	0.16	0.03	84%		0.4		
<b>V</b>	0.4 $\pm$ 0.06	0.34-0.46	0.33	0.07	83%				
<b>Zn</b>	5.7 $\pm$ 1.9	3.74-7.42	2.51	3.20	44%		4.2-6.1	6	

312 <sup>a</sup>: total bulk deposition from Bergametti et al. (1987 and 1992) and Remoudaki et al. (1991)

313 <sup>b</sup>: total bulk deposition from Ridame et al. (1999)

314 <sup>c</sup>: total bulk deposition from Guieu et al. (2010) and Markaki et al. (2010)

315 <sup>d</sup>: total wet deposition from Löye-Pilot et al. (1990)

316 \* data obtained between jun. 2001 and May 2003

317

318

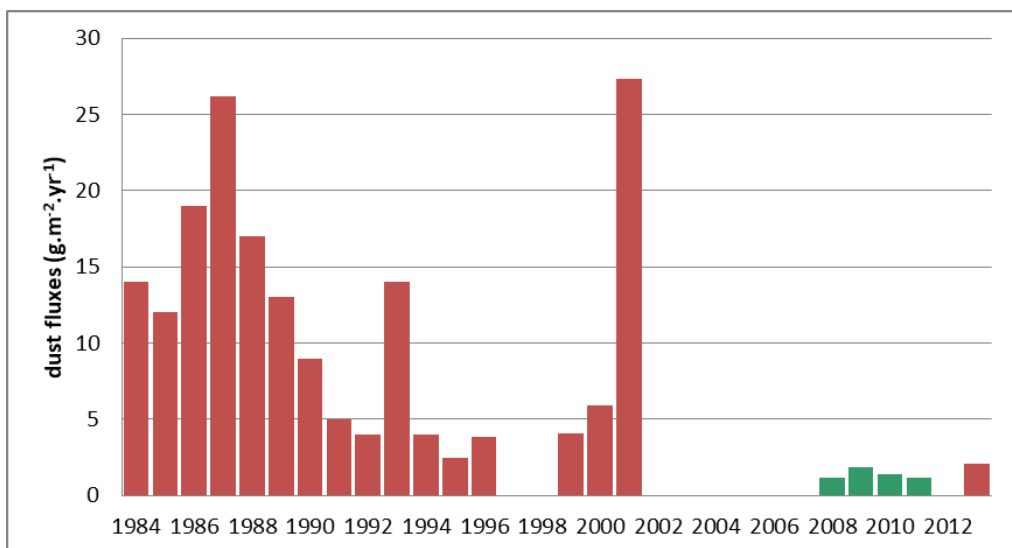
319

320

### 321        **3.3.    Mineral dust deposition fluxes**

322    The annual deposition fluxes of soil dust have been estimated from Al fluxes, considering an  
323    amount of Al of 7% (Guieu et al., 2010). The results show that the mean annual dust flux ranges  
324    from 1.39 to 1.94 g m<sup>-2</sup> y<sup>-1</sup>. Typically, 70% of the annual flux is related to 3 or 4 dust deposition  
325    events during the year, in agreement with the sporadic pattern of dust input over the year  
326    (Löye-Pilot et al., 1996). For example, a weekly maximum of 0.82 g m<sup>-2</sup> w<sup>-1</sup> is recorded during  
327    the last week of April 2009, representing 44% of the total flux for this year. It is well known  
328    that the intense dust events lead to a very high intra and inter-annual variability. Al deposition  
329    data recording in Corsica show a range of dust fluctuation for the period 1985-2002 in Corsica  
330    being to 4 to 28 g m<sup>-2</sup> y<sup>-1</sup> (Guieu et al., 2010), higher value being always associated with very  
331    intense events (>10 g m<sup>-2</sup>). Our values between 2008 and 2011 are lower than the range  
332    previously measured between the 1980's and early 2000's, probably because no intense dust  
333    event (>1 g m<sup>-2</sup>) has been recorded during the sampling period (Figure 3). This trend is  
334    consistent with the low annual deposition mass fluxes observed by Vincent et al. (2016)  
335    recorded in Corsica and more generally in the western Mediterranean between 2011 and 2013  
336    (max 2.1 g m<sup>-2</sup> yr<sup>-1</sup>). This result is also coherent with the decreasing trend in PM<sub>10</sub>  
337    concentrations over the Mediterranean region due to the decrease of dust contribution (Pey  
338    et al., 2013). As mentioned by Moulin et al. (1997) and Pey et al. (2013), this is probably due  
339    to the variation in large scale atmospheric circulation affecting dust atmospheric contents  
340    (lower values of the NAO indices during the last two decades). This trend could be also is  
341    related to the low dust activity period in Sahara during the 2000's in comparison to 1970-1990  
342    proposed by Evan et al. (2016) from wind variability pattern. However, the kind of deposition  
343    collectors and the sampling sites being different, we cannot exclude effects of sampling  
344    conditions on the obtained results.

345



346  
347  
348  
349  
350

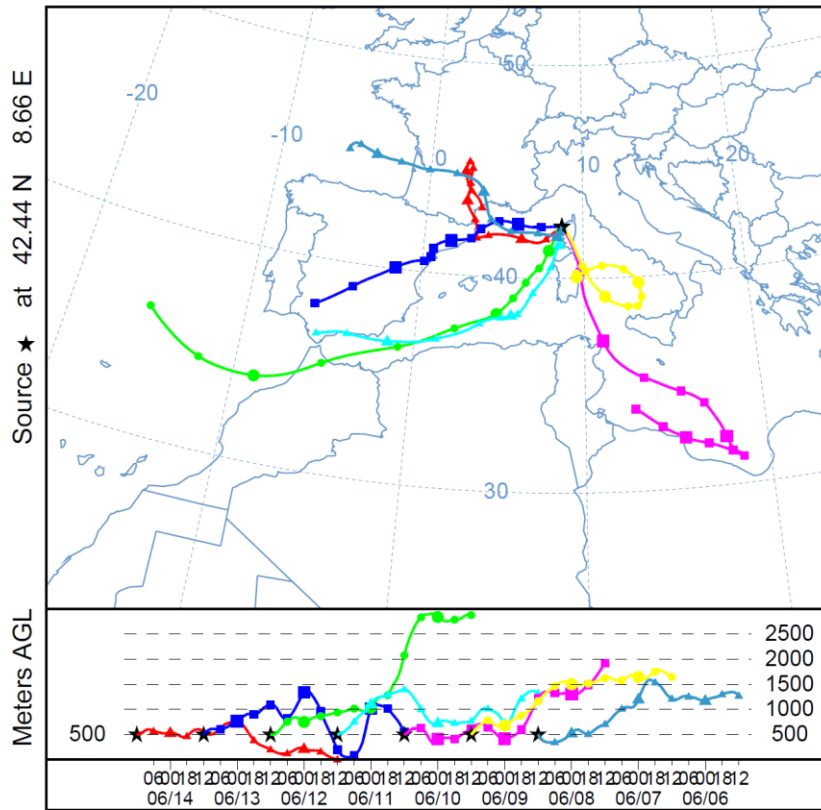
Figure 3: Time-series of dust fluxes ( $\text{g m}^{-2} \text{an}^{-1}$ ) at various locations in Corsica issued from Löye-Pilot and Martin (1996) for years between 1984 and 1994, from Ridame et al. (1999) for 1995 and 1996, from Guieu et al. (2010) for 2001-2002, from Vincent et al. (2016) for 2013 (all in red) and from this work for 2008-2011 (in green).

### 351 **3.4. The case of high deposition events**

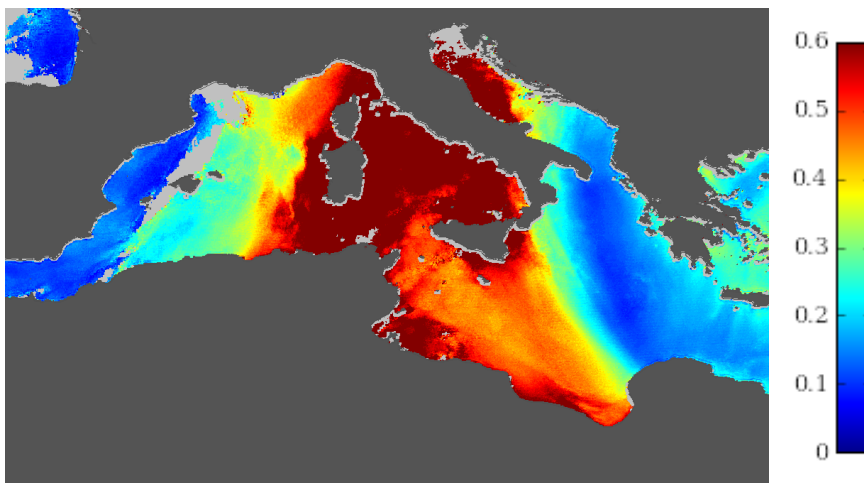
352 Over our sampling period (March 2008-October 2011), the average weekly dust deposition is  
 353  $0.028 \pm 0.07 \text{g m}^{-2} \text{w}^{-1}$ . In order to identify the outlier dust events in the data set, we selected  
 354 the samples with weekly fluxes higher than the last 95<sup>th</sup> percentile of data, i.e. the 5 % of  
 355 highest values. Thus, weekly dust fluxes  $> 0.104 \text{g m}^{-2} \text{w}^{-1}$  are considered as the extreme dust  
 356 events. From this threshold, 12 samples are isolated and correspond to 10 dust events (2  
 357 events concern two successive sampling periods in April 2009 and June 2010). All these events  
 358 correspond to wet deposition periods (Figure 1). Observations of remote sensing data from  
 359 MODIS or SEVIRI confirm that these events are due to intense Saharan dust plumes associated  
 360 with clouds (not shown). Eight of these events happened in spring (between March and June),  
 361 1 in fall and 1 in winter, in agreement with the seasonal pattern of dust plumes over the  
 362 western Mediterranean (Moulin et al., 1988) and in particular in Corsica (Bergametti et al.,  
 363 1989; Salvador et al., 2014). The first week of one of the two dust events which fall in two  
 364 sampling periods corresponds also with the high episode of As deposition ( $0.1 \text{mg m}^{-2} \text{wk}^{-1}$ )  
 365 recorded in June 2010. This weekly As flux represents the annual flux measured in a remote  
 366 environment like Scandinavia forest ( $0.1 \text{mg m}^{-2} \text{yr}^{-1}$  on average between 2002-2005;  
 367 Hovmand et al., 2008). It is much larger than the weekly fluxes recorded in an urban  
 368 environment as Venice where the reported fluxes range from 0.7 to  $367 \mu\text{g m}^{-2} \text{wk}^{-1}$  between

369 2005-2010 (Morabito et al., 2014). The As/Al ratio (0.011) for this event shows a large  
370 enrichment in As (x16) in comparison to the average of other intense dust events ( $7.10^{-4}$ ),  
371 which are in agreement with the crustal ratio (Mason and Moore, 1982). The identified  
372 sources of atmospheric particulate As are coal-fired industries, waste-incineration, oil refining,  
373 mining and fossil fuel combustion (Wai et al., 2016). In the given sample, an enrichment in  
374 comparison to the other intense dust events is also observed for P (x12), Sr (x9), Cu and Zn  
375 (x6) whereas no significant enrichment is observed during the second sampling week of the  
376 dust event. Besides dust and marine aerosol, the biomass burning and fossil fuel combustion  
377 are the main sources of anthropogenic Cu, P, Sr and Zn (Mahowald et al., 2008; Nava et al.,  
378 2015). Moreover, the particulate filter corresponding with this event was brown-grey,  
379 showing a probable mixing between dust and black carbon (not shown). During the As-rich  
380 deposition week, the back-trajectories show that the air masses came mainly from South in  
381 concomitance with a high dust intrusion in the western Mediterranean basin (Figure 4), no  
382 intense biomass burning event is recorded during this period on the pathways of back-  
383 trajectories. A mixing with dust and anthropogenic aerosol, rich in metals, over Mediterranean  
384 has been already observed (Dulac et al., 1987; Heimbürger et al., 2016). Our observations  
385 suggest that either deposition from a likely local combustion source occurred during the week  
386 of the dust deposition event or the deposited dust was mixed with aerosols issued from  
387 combustion source along its transport over Africa or Mediterranean.

NOAA HYSPLIT MODEL  
 Backward trajectories ending at 1200 UTC 14 Jun 10  
 GDAS Meteorological Data



388



389

390 **Figures 4: (a) Pathways of 3-day back-trajectories ending at 500 m at the sampling site at noon from NOAA HYSPLIT model**

391 **for the week of As-rich event and (b) MSG/SEVIRI daily (daytime) mean aerosol optical depth over Ocean for the 10<sup>th</sup> of**

392 **June 2010 in agreement with the intrusion of an intense Saharan dust event during this week.**

393

394

395



396 The dust flux associated to these most intense dust deposition events represents 56% of the  
397 total dust flux on the 3.5 years of recording. The contribution of dust events on the fluxes Fe  
398 and Si represents 52% and 57% of their total fluxes respectively. Our results confirm the  
399 important role of these sporadic dust events on the inputs of these elements. In agreement  
400 with previous observations, Si and Fe fluxes present also a good correlation with Al fluxes ( $R^2=$   
401  $0.97$  and  $0.96$ , respectively) and mean mass ratios ( $Si/Al = 2.5$  and  $Fe/Al = 0.57$ ) are typical of  
402 Saharan dust (Formenti et al., 2008 and 2011) and of transported dust in European sites  
403 (Alastuey et al., 2016), supporting more generally the important role of dust deposition on Si  
404 and Fe.

405 For N and P, the contribution of the outlier dust events is lower and reaches 10 and 15%  
406 respectively, and even 11% for P if the As-dust mixed event is excluded. That means that other  
407 sources than soil dust dominate the fallouts of these species (Figure 1). However, a peak in N  
408 and P fluxes is systematically observed during high dust events, showing at the same time that  
409 intense dust deposition is also a source of these elements. The reactivity between dust and  
410 nitric acid previously observed in Mediterranean (e.g. Puteaud et al., 2004) could explain the  
411 link between dust fluxes and N fluxes. For trace metals, the high dust deposition events  
412 represent around 1/3 of total fluxes for Cr, Mn, Ni and V, whereas the contribution is low for  
413 As (10% without the intense event), Cu (16% and even 12% excluding As-dust mixed event)  
414 and Zn (9% and even 6% excluding As-dust mixed event). Keeping in mind that no high dust  
415 deposition event  $>1 \text{ g m}^{-2}$  has been recorded during our 2008-2011 period of sampling, our  
416 data confirm that African dust wet deposition constitutes the major atmospheric source for  
417 Fe and Si to the northwestern Mediterranean and an important source for Cr, Mn, Ni and V  
418 (1/3 of their total fluxes).

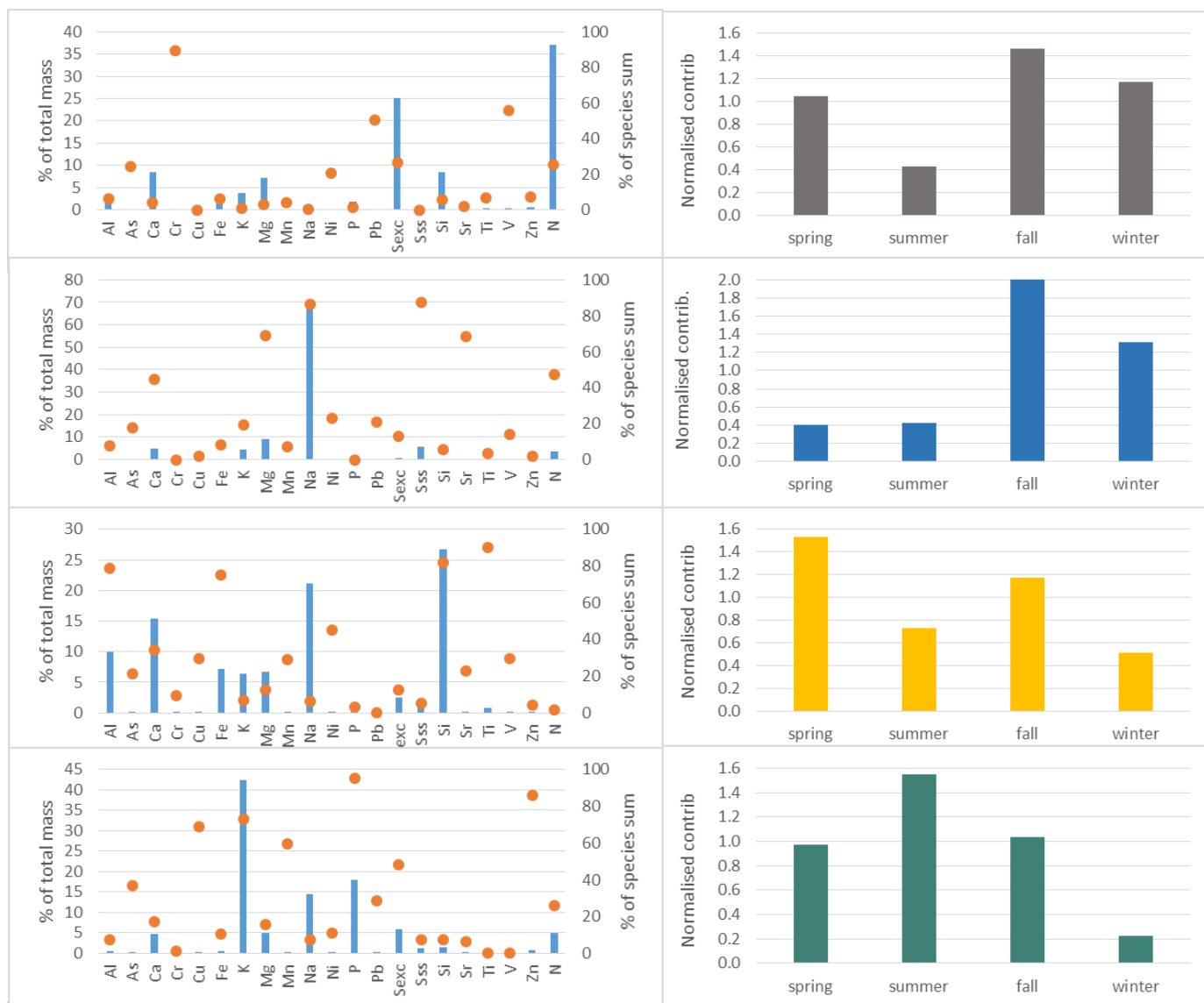
419

### 420 **3.5. Source apportionment and background deposition**

421 In order to perform a source apportionment by the PMF method, we excluded the 12 samples  
422 corresponding to the high African dust deposition events in order to address background  
423 atmospheric deposition. We evaluated PMF solutions with two to six factors. Finally, a solution  
424 with 4 factors has been chosen since it is the optimum solution coupling a good agreement  
425 with our understanding of sources identification and the indicator of PMF optimization. The  
426 4-factor solution was the most stable with a sharper decrease in the  $Q/Q_{exp}$  trend and a

427 constant global minimum Q value among 100 random runs. In terms of the stability of the  
428 PMF analysis, all factors of the 4-factor solution were reproduced in 100% of bootstrap runs,  
429 demonstrating that this solution was stable. No correlation between 4 factors has been  
430 observed, indicating that they represented distinct sources. The 4-factor solution enables to  
431 apportion the results between 4 sources: a dust factor (related to Si, Al, Ca, Fe and Ti), a marine  
432 aerosol factor (related to Na, Mg, Sr), an anthropogenic source factor (related to Cr, Pb, V, N,  
433 Sexc) and a biomass burning factor (related to K, P, Zn, Cu and Mn) (Figure 5). This source  
434 identification is based on the presence of tracer elements as well as on the ratio of the  
435 elements in the source profile. The source identification was also supported by the seasonal  
436 contributions of each source to the atmospheric fluxes shown in Fig. 5. The identification of  
437 factors was supported by the previous works on source apportionment of aerosol particles in  
438 the Mediterranean (Calzolari et al., 2015, Becagli et al., 2012 and 2017). However, even if the  
439 oil-combustion source (rich in Ni-V) has been typically observed in the central Mediterranean,  
440 no PMF solution (2- to 6-factor solutions) did enable us extracting a Ni-V factor, corresponding  
441 to a ship plume signature. The heavy oil combustion signature could be contained in the  
442 anthropogenic factor. However, the typical V/Ni ratio of ship emissions are between 2.5 and  
443 4.5 (Becagli et al., 2012), whereas this ratio is higher than 8 in the anthropogenic factor,  
444 suggesting that the ship plumes are dominant in this factor. Even if this source could be  
445 important for aerosol concentrations over the Mediterranean Sea (Becagli et al., 2017), it does  
446 not seem to be important for deposition in Corsica. The marine factor is marked by Na, Sss,  
447 Mg and Sr, with at least 60% of their fluxes corresponding to this source. The elemental ratio  
448 obtained for this source ( $Mg/Na = 0.13$ ;  $K/Na = 0.064$ ;  $Ca/Na = 0.070$ ,  $Sr/Na = 8.5 \times 10^{-4}$ ) are in  
449 agreement with the typical elemental ratio in seawater ( $Mg/Na = 0.12$ ;  $K/Na = 0.037$ ;  
450  $Ca/Na = 0.038$ ;  $Sr/Na = 7 \times 10^{-4}$ ; Bowen, 1979). It is known that sea salt aerosol concentrations  
451 are a function of surface wind speeds (O'Downd et al., 1993). The seasonal contribution of this  
452 source is consistent with a larger wind production in fall and winter, with a maximum of  
453 deposition in agreement with the maximum of rain in fall. Na represents on the total mass at  
454 least 15% for dust and biomass burning factors due to the high influence of marine  
455 environment on the Corsica Island. The factor identified as dust source, marked by Al, Fe, Si,  
456 Ti, is in agreement with the typical seasonal variation of dust deposition in Corsica with a  
457 maximum in spring and in fall (Bergametti et al., 1989). Moreover, the elemental ratios ( $Si/Al$   
458  $= 2.7$ ;  $Fe/Al = 0.72$ ;  $Ti/Fe = 0.12$ ) correspond to a Saharan dust signature ( $Si/Al$  between 2 and

459 4 and Ti/Fe between 0.1 and 0.15; Formenti et al., 2014), but also with the typical ratio found  
460 in PM10 in remote area in Mediterranean (Alastuey et al., 2016). The biomass burning/waste  
461 source is mainly characterized by Cu, K, P and Zn. K is commonly associated to waste/biomass  
462 burning or wood combustion (Dall'osto et al., 2013, Nava et al., 2015). The maximum of this  
463 source deposition in summer, in spite of a minimum of rain, corresponds with the intense  
464 forest fires observed in the Mediterranean region in this period, and which the extend impacts  
465 all the basin (Bossioli et al., 2016). Finally, Cr, Pb, V, Sexc and N are the characterizing elements  
466 found in the anthropogenic source. Even with >4-factor solutions, no profile distinguishing N,  
467 Sexc and metals is emphasized by PMF, suggesting a common source, at least geographically.  
468 Thus, the major contribution of N and Sexc in mixing with metals suggest that this source  
469 correspond with the secondary aerosols formed in air masses issued from combustion sources  
470 (traffic, industrial). The two sources of combustion identified by PMF, i.e. biomass burning and  
471 anthropogenic sources, have previously been observed in background aerosols in another  
472 remote site in Corsica (Arndt et al., 2017; Claeys et al. 2017).  
473



475 **Figure 5: PMF-derived profiles of the four sources identified. From top to bottom: (a) anthropogenic, (b) marine, (c) dust**  
 476 **and (d) biomass burning including fraction of total mass (blue columns) and fraction of elemental sum (orange circles) for**  
 477 **the various elements (Left side). Normalized seasonal contributions of these four respective factors, excluding the 10 most**  
 478 **intense dust events (Right side).**

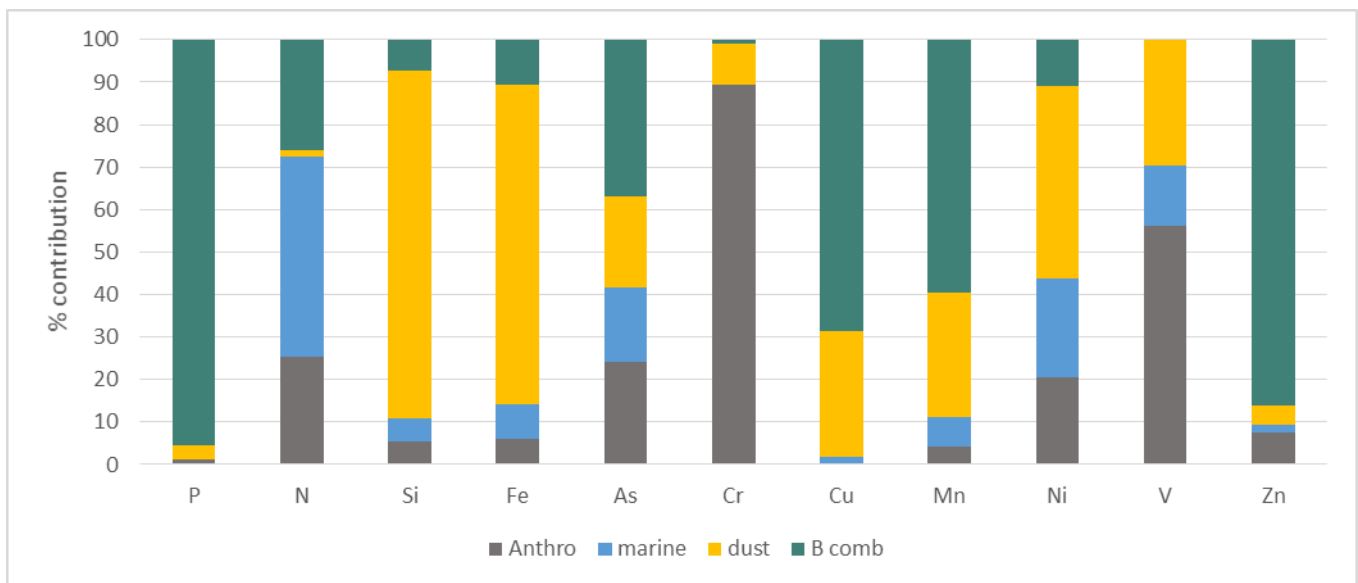
479  
 480 In Figure 6, we show the relative contribution from the identified sources to background  
 481 deposition flux of nutrients and trace metals. The results show that the combustion sources  
 482 (biomass burning or anthropogenic) predominates in the background inputs of major  
 483 nutrients and TMs, except Fe and Si. Even for background deposition, the source  
 484 apportionment of Fe and Si is quasi-similar to Al (correlation coefficient is close to 1 for the  
 485 elemental fluxes even out of intense events and ratio Si/Al and Fe/Al are characteristics of  
 486 mineral dust). These results suggest that even if the PMF apportionment source distributes

487 the fluxes from the 4 sources, in all the cases, the fluxes of Fe and Si are associated to mineral  
488 dust sources, most probably Saharan dust.

489 Concerning major nutrients, P deposition is highly associated to biomass burning inputs out  
490 of the most intense dust deposition events. Considering that the dust deposition accounts for  
491 15% of the total P deposition flux (incl. intense dust deposition events + background  
492 deposition), almost 85% of P inputs are associated to the deposition of biomass  
493 burning/waste/wood-related aerosol. This confirms the importance to consider the biomass  
494 combustion source to estimate the role of this element on the marine environment in the  
495 Mediterranean. For N deposition, the inputs associated to marine sources are quasi-similar to  
496 the inputs from combustion sources. Thus, almost 50% of N fluxes is explained by the marine  
497 source. Several works observed that the depletion of chloride (Cl) and the simultaneous  
498 occurrence of  $\text{NO}_3^-$  in sea salt aerosol particles is due to the reaction between NaCl and  $\text{HNO}_3$   
499 when maritime and anthropogenic air masses are mixed, in Mediterranean environments  
500 (Sellegrri et al., 2001; Bardouki et al., 2003; Pey et al., 2009) and in particular in Corsica (Claeys  
501 et al., 2017). The contribution of marine source to N deposition is probably due to the  
502 deposition of these processed sea-salt particles. In the case of the anthropogenic source  
503 factor, the good correlation obtained between N and  $\text{Sexc}$  supports a common origin which is  
504 probably associated to the inorganic secondary aerosol, i.e. ammonium sulfate. Indeed, the  
505 ammonium sulfate aerosols are currently observed in Corsica due to regional transport (Arndt  
506 et al., 2017) and generally in the Mediterranean remote sites (e.g. Calzolari et al., 2015). As  
507 stated previously, the using of N speciation is limited by the preservation conditions of our  
508 samples. However, we observed a concomitance between the highest deposited mass of  $\text{NH}_4^+$   
509 and  $\text{Sexc}$ , and of  $\text{NO}_3^-$  and Na (See supplement). It reinforces our conclusion on a partition  
510 between N as  $\text{NH}_4^+$  mainly associated to ammonium sulfate for the anthropogenic factor, and  
511 N as  $\text{NO}_3^-$  present as  $\text{NaNO}_3$  for the marine factor. It is known that the deposition efficiency of  
512 particles in the coarse mode, as sea salts, is higher than the one of fine particles, as inorganic  
513 secondary aerosols. Our results suggest that the addition of nitrate on sea salt particles could  
514 be a key process in controlling the N atmospheric deposition fluxes to the Mediterranean  
515 surface waters. Recent works suggest that a large part of nitrogen associated to anthropogenic  
516 secondary aerosol could be soluble organic nitrogen (Violaki et al., 2015). Thus, the observed  
517 diversity in sources of deposited N could also mean a difference in N speciation in the fallout  
518 (inorganic vs organic).

519 For trace metals, the marine source present the lowest contribution. The biomass  
 520 burning/waste source is clearly predominant for Cu, Mn and Zn, whereas atmospheric fluxes  
 521 of Cr and Ni are largely linked to the anthropogenic source. Fu et al. (2017) show that the Cr  
 522 deposition in Cape Corsica, even during intense dust event is originated from an  
 523 anthropogenic source, suggesting a contamination by a local source. Even if the Cape Corsica  
 524 and our sites of deposition measurements are distant by about 100 km, both suggest that Cr  
 525 deposition is controlled by an anthropogenic source. For Zn, Guieu et al. (2010) also showed  
 526 a large contribution of non-dust source. Our work enables to support their conclusions and to  
 527 identify a biomass combustion source rather than a fossil fuel or industrial origin. It appears  
 528 that the deposition of Cu, Mn, Ni and V is influenced at least for 20% by dust deposition out  
 529 of intense events. That means that for these trace metals, the natural dust inputs can  
 530 represent up to 50% of annual fluxes.

531



533 **Fig. 6: Relative contribution of each of the 4 identified factors (Anthro= anthropogenic, marine, dust and B comb= biomass**  
 534 **combustion) to the “background” mass fluxes of nutrients and TMs (i.e. excluding the 12 most intense African dust**  
 535 **deposition samples out of 195 samples).**

536

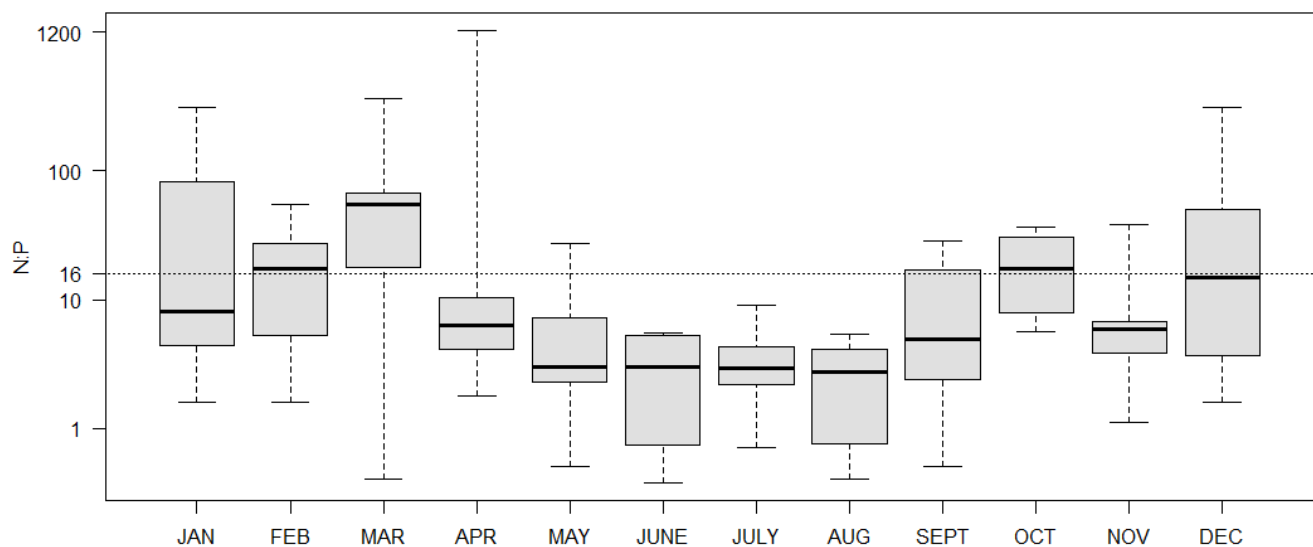
### 537 **3.6. Biogeochemical implications**

538 The typical N:P molar ratio in seawater required by marine phytoplankton corresponds to the  
 539 Redfield ratio of 16. This ratio is generally higher in Mediterranean surface seawater, with  
 540 values ranging from 20 to 100 on the basin (Ribera d’Alcala et al., 2003). The atmospheric  
 541 input to the Mediterranean Sea displays a high N:P ratio for dissolved or soluble inorganic

542 forms (Herut and Krom, 1996), which could be one possible reason of the high N:P ratio in  
543 Mediterranean deep sea waters (Markaki et al., 2010; Krom et al., 2010).

544 In our data set, the yearly deposition mass fluxes measured for N and P are quasi equivalent  
545 ( $0.14\text{-}0.15\text{ g m}^{-2}\text{ yr}^{-1}$ ; Table 1). However, weekly measurements show a very large variability in  
546 P fluxes, contrary to N. Hence, a large variability in the N:P molar ratio is observed in the  
547 atmospheric inputs at short time scales. A mean value of 35 is observed for the molar ratio  
548 but the weekly ratio ranges from 0.4 to 1220. The observed N enrichment in comparison to  
549 the Redfield ratio is in agreement with previous observations showing a preponderance of N  
550 relative to P in the atmospheric deposition over the Mediterranean Sea (Markaki et al., 2010).  
551 However, a detailed analysis shows that the atmospheric ratio is equal or higher than Redfield  
552 ratio only for 25% of samples, and higher than 160 only for 3 samples (4%). This value reaches  
553 36% for the wet periods. The higher ratio observed in wet deposition could be linked to a  
554 wash-out effect of the gaseous N species (as  $\text{NO}_x$ ,  $\text{NH}_3$ ) by rain (Ochoa-Hueso et al., 2011).  
555 The intense dust events present an average N:P ratio of 3.5, which is lower than previously  
556 reported for dust deposition (between 30 and 70; Morales-Baquero et al., 2013). However,  
557 this value is consistent with the typical N:P ratio in Saharan dust aerosols which is around to  
558 2.5. The highest N:P ratio are generally due to the reactivity of dust aerosol with gaseous nitric  
559 acid to form nitrate on dust particles (Desboeufs et al., 2014). Our data suggest that the effect  
560 of mixing between dust and nitric acid did not commonly affect atmospheric dust deposited  
561 in Corsica, except maybe during certain high dust deposition. On the contrary, the mixing  
562 between sea salt and nitric acid identified with the source apportionment could be a source  
563 of N during the fall and winter period, when the biomass burning source is negligible. It  
564 appears also that the lowest N:P ratio values are mainly observed from May to September  
565 (Figure 7). During this period, the atmospheric deposition becomes the main sources of  
566 nutrients since the Mediterranean is highly stratified and the surface is depleted in nutrients.  
567 Thus, in these conditions, the atmospheric inputs will be deficient in N relative to  
568 phytoplankton requirements. Studies show that phytoplankton growth in western  
569 Mediterranean waters is usually limited by a lack of phosphate, rather than nitrate in summer  
570 (Lazzari et al., 2016; Richon et al., 2018a), even if phosphorus addition experiments have  
571 indicated also N limitation in this period (Tanaka et al., 2011). Our results suggest that the role  
572 of atmospheric aerosol input will be rather favorable in case of P-starvation of surface  
573 seawater. However, even if the N:P ratio from this study were obtained with comparable

574 deposition collectors than previous literature (e.g. Markaki et al., 2010), it has to be kept in  
 575 mind the deposition collectors were not optimized for gaseous N fluxes measurements, and  
 576 the N:P ratio could be underestimated. The temporal evolution of marine N and P  
 577 concentrations since 1985 has shown a high sensitivity to anthropogenic atmospheric  
 578 deposition and they are expected to decline in the coming decades due to mitigation/control  
 579 of pollutant emissions (Moon et al. 2016). Due to the high contribution of anthropogenic  
 580 deposition sources on atmospheric P fluxes emphasized by our study, it is important to include  
 581 precise anthropogenic P emissions inventories to estimate the impact of atmospheric  
 582 deposition on carbon fluxes and phytoplankton biomass in the future.  
 583



585 **Figure 7: Box plots of monthly molar N:P ratio in deposition samples, showing the third quartile (Q3) and first quartile (Q1)**  
 586 **range of the data and minimum and maximum of data. For the sake of comparison, The N:P scale is logarithmic and the**  
 587 **Redfield ratio is displayed.**  
 588

#### 589 4. Conclusion

590 In a context of anthropogenic changes, in order to assess how the evolution of chemical  
 591 atmospheric forcing will modify the marine nutrient cycling, it is crucial to distinguish between  
 592 anthropogenic vs natural atmospheric inputs of nutrients to the oligotrophic Mediterranean  
 593 surface waters. We monitored elemental atmospheric deposition on a weekly basis over 3.5-  
 594 years (March 2008-October 2011) at a coastal site on the western coast of Corsica. The  
 595 contribution of 4 different source types to the fallout of nutrients and trace metals was  
 596 determined by statistical PMF method, namely desert dust, sea-salt, anthropogenic activities,



597 and biomass combustion sources. The data show that Si and Fe fluxes are typically related to  
598 African dust deposition, with fluxes dominated by high dust deposition events. A typical Si/Al  
599 ratio of 2.5 is obtained whatever the samples. That shows that Al is a good proxy to estimate  
600 the Si fluxes in Mediterranean region since Si is often not measured when X-Ray fluorescence  
601 spectrometry is not available due its lost by HF digestion during the protocol of chemical  
602 analysis. Our results on the mineral dust fallout is of the same order of magnitude that of 2013  
603 at another site in Corsica (Vincent et al., 2016) and confirm the fact that dust deposition has  
604 strongly decreased in Corsica in the recent years compared to the 1980's and 1990's, with no  
605 observed occurrence of a high dust deposition event larger than  $1 \text{ g m}^{-2}$  in 2008-2011 (this  
606 work) and 2013 (Vincent et al., 2016).

607 Atmospheric fluxes of Cu, Mn, Ni and V are also associated at least at 50% to mineral dust  
608 deposition, whereas half of atmospheric fluxes is issued either from biomass burning particles  
609 deposition (Cu and Mn), either from fossil fuel combustion (V), either both (Ni). The  
610 anthropogenic/combustion sources govern the atmospheric fluxes of major nutrient N and P,  
611 with a predominance of biomass combustion source for P and secondary aerosols for N. Dust  
612 deposition is contributing around 15% of deposited P at the yearly time scale. Confirming  
613 recent model results that desert dust is not dominant on atmospheric P fluxes (Richon et al.,  
614 2018b), our result show that these combustion sources need to be considered in P deposition  
615 modelling. Finally, Zn or Cr deposition is very largely associated to continuous combustion  
616 sources.

617 This work is a first tentative assessment of the origin of nutrients and trace metals deposited  
618 in the western Mediterranean. Of course, our study is not sufficient to apprehend the spatial  
619 variability of the influence of the identified source types over the basin. It needs to be  
620 supported by other studies of source apportionment on deposition samples in the region.

621

#### 622 *Acknowledgements:*

623 *The authors wish to warmly thank Pasquale Simeoni from Parc Naturel Régional de Corse who*  
624 *made possible the weekly samples collection and the maintenance of sampling site. This study*  
625 *received financial support from the French ANR through the project DUNE and from the*  
626 *MISTRALS programme funded by INSU, ADEME, CEA and Météo-France. This study contributes*  
627 *to WP5 on Atmospheric Deposition of the MISTRALS/ChArMEx project. The authors want to*  
628 *thank Rémi Losno for his involvement in the installation of deposition collectors, and the staff*  
629 *of the Parc Naturel Régional de Corse for assistance in sampling.*

- 631 Alastuey, A., Querol, X., Aas, W., Lucarelli, F., Pérez, N., Moreno, T., Cavalli, F., Areskoug, H., Balan, V.,  
632 Catrambone, M., Ceburnis, D., Cerro, J. C., Conil, S., Gevorgyan, L., Hueglin, C., Imre, K., Jaffrezo, J.-  
633 L., Leeson, S. R., Mihalopoulos, N., Mitisinkova, M., O'Dowd, C. D., Pey, J., Putaud, J.-P., Riffault, V.,  
634 Ripoll, A., Sciare, J., Sellegri, K., Spindler, G., and Yttri, K. E.: Geochemistry of PM<sub>10</sub> over Europe during  
635 the EMEP intensive measurement periods in summer 2012 and winter 2013, *Atmos. Chem. Phys.*, 16,  
636 6107-6129, <https://doi.org/10.5194/acp-16-6107-2016>, 2016.
- 637 Amato, F., Alastuey, A., Karanasiou, A., Lucarelli, F., Nava, S., Calzolari, G., Severi, M., Becagli, S.,  
638 Gianelle, V. L., Colombi, C., Alves, C., Custadio, D., Nunes, T., Cerqueira, M., Pio, C., Eleftheriadis, K.,  
639 Diapouli, E., Reche, C., Minguillon, M. C., Manousakas, M. I., Maggos, T., Vratolis, S., Harrison, R. M.,  
640 and Querol, X.: AIRUSE-LIFE+: a harmonized PM speciation and source apportionment in  
641 five southern European cities, *Atmos. Chem. Phys.*, 16, 3289-3309, doi:10.5194/acp-16-3289-2016,  
642 2016.
- 643 Arndt, J., Sciare, J., Mallet, M., Roberts, G. C., Marchand, N., Sartelet, K., Sellegri, K., Dulac, F., Healy, R.  
644 M., and Wenger, J. C.: Sources and mixing state of summertime background aerosol in the north-  
645 western Mediterranean basin, *Atmos. Chem. Phys.*, 17, 6975-7001, doi:10.5194/acp-17-6975-2017,  
646 2017.
- 647 Bardouki, H., Liakakou, H., Economou, C., Sciare, J., Smolik, J., Zdimal, V., Eleftheriadis, K., Lazaridis, M.,  
648 Dye, C., and Mihalopoulos, N.: Chemical composition of size-resolved atmospheric aerosols in the  
649 eastern Mediterranean during summer and winter, *Atmos. Environ.*, 37, 195-208,  
650 doi:10.1016/S1352-2310(02)00859-2, 2003.
- 651 Becagli, S., Sferlazzo, D. M., Pace, G., di Sarra, A., Bommarito, C., Calzolari, G., Ghedini, C., Lucarelli, F.,  
652 Meloni, D., Monteleone, F., Severi, M., Traversi, R., and Udisti, R.: Evidence for heavy fuel oil  
653 combustion aerosols from chemical analyses at the island of Lampedusa: a possible large role of ships  
654 emissions in the Mediterranean, *Atmos. Chem. Phys.*, 12, 3479-3492, doi:10.5194/acp-12-3479-  
655 2012, 2012.
- 656 Becagli, S., Anello, F., Bommarito, C., Cassola, F., Calzolari, G., Di Iorio, T., di Sarra, A., Gómez-Amo, J.-  
657 L., Lucarelli, F., Marconi, M., Meloni, D., Monteleone, F., Nava, S., Pace, G., Severi, M., Sferlazzo, D.  
658 M., Traversi, R., and Udisti, R.: Constraining the ship contribution to the aerosol of the central  
659 Mediterranean, *Atmos. Chem. Phys.*, 17, 2067-2084, doi:10.5194/acp-17-2067-2017, 2017.
- 660 Bergametti, G., Apports de matière par voie atmosphérique à la Méditerranée Occidentale: aspects  
661 géochimiques et météorologiques, PhD, 296 pp., Univ. Paris VII, Paris, 1987.
- 662 Bergametti, G., Dutot, A. L., Buat-Ménard, P., Losno, R., and Remoudaki, E.: Seasonal variability of the  
663 elemental composition of atmospheric aerosol particles over the Northwestern Mediterranean,  
664 *Tellus*, 41B, 353-361, doi:10.1111/j.1600-0889.1989.tb00314.x, 1989.
- 665 Bergametti, G., Remoudaki, E., Losno, R., Steiner, E., Chatenet B., and Buat-Ménard, P.: Sources,  
666 transport and deposition of atmospheric phosphorus over the northwestern Mediterranean, *J.*  
667 *Atmos. Chem.*, 14, 501-513, doi:10.1007/BF00115254, 1992.
- 668 Bethoux J.-P., Courau, P., Nicolas, E., Ruiz-Pino, D.: Trace-metal pollution in the Mediterranean-sea.  
669 *Oceanol. Acta*, 13, 481-488, 1990.
- 670 Bonnet, S., and Guieu, C.: Atmospheric forcing on the annual iron cycle in the western Mediterranean  
671 Sea: A 1-year survey, *J. Geophys. Res.-Oceans*, 111, 2006.
- 672 Bossioli, E., Tombrou, M., Kalogiros, J., Allan, J., Bacak, A., Bezantakos, S., Biskos, G., Coe, H., Jones, B.  
673 T., Kouvarakis, G., Mihalopoulos, N., and Percival, C. J.: Atmospheric composition in the Eastern  
674 Mediterranean: Influence of biomass burning during summertime using the WRF-Chem model,  
675 *Atmos. Environ.*, 132, 317-331, doi:10.1016/j.atmosenv.2016.03.011, 2016.

- 676 Bowen, H. J. M.: Environmental chemistry of the elements, Academic Press, 1979.
- 677 Calzolari, G., Nava, S., Lucarelli, F., Chiari, M., Giannoni, M., Becagli, S., Traversi, R., Marconi, M., Frosini,  
678 D., Severi, M., Udisti, R., di Sarra, A., Pace, G., Meloni, D., Bommarito, C., Monteleone, F., Anello, F.,  
679 and Sferlazzo, D. M.: Characterization of PM10 sources in the central Mediterranean, *Atmos. Chem.*  
680 *Phys.*, 15, 13939-13955, doi:10.5194/acp-15-13939-2015, 2015.
- 681 Chester, R., Nimmo, M., and Keyse, S.: The influence of saharan and middle eastern desert-derived  
682 dust on the trace metal composition on Mediterranean aerosols and rainwaters: an overview, in: *The*  
683 *impact of Desert dust across the Mediterranean*, edited by: Guerzoni, S., and Chester, R., Kluwer  
684 Academic Publishers, Dordrecht, 253-273, 1996.
- 685 Claeys, M., Roberts, G., Mallet, M., Arndt, J., Sellegri, K., Sciare, J., Wenger, J., and Sauvage, B.: Optical,  
686 physical and chemical properties of aerosols transported to a coastal site in the western  
687 Mediterranean: a focus on primary marine aerosols, *Atmos. Chem. Phys.*, 17, 7891-7915,  
688 doi:10.5194/acp-17-7891-2017, 2017.
- 689 Dall'Osto, M., Querol, X., Amato, F., Karanasiou, A., Lucarelli, F., Nava, S., Calzolari, G., and Chiari, M.:  
690 Hourly elemental concentrations in PM2.5 aerosols sampled simultaneously at urban background  
691 and road site during SAPUSS – diurnal variations and PMF receptor modelling, *Atmos. Chem. Phys.*,  
692 13, 4375-4392, doi:10.5194/acp-13-4375-2013, 2013.
- 693 Desboeufs, K., Leblond, N., Wagener, T., Bon Nguyen, E., and Guieu, C.: Chemical fate and settling of  
694 mineral dust in surface seawater after atmospheric deposition observed from dust seeding  
695 experiments in large mesocosms, *Biogeosci.*, 11, 5581-5594, doi:10.5194/bg-11-5581-2014, 2014.
- 696 Diapouli, E., Manousakas, M. I., Vratolis, S., Vasilatou, V., Pateraki, S., Bairachtari, K. A., Querol, X.,  
697 Amato, F., Alastuey, A., Karanasiou, A. A., Lucarelli, F., Nava, S., Calzolari, G., Gianelle, V. L., Colombi,  
698 C., Alves, C., Custodio, D., Pio, C., Spyrou, C., Kallos, G. B., and Eleftheriadis, K.: AIRUSE-LIFE +:  
699 estimation of natural source contributions to urban ambient air PM10 and PM2.5 concentrations in  
700 southern Europe - implications to compliance with limit values, *Atmos. Chem. Phys.*, 17, 3673-3685,  
701 doi:10.5194/acp-17-3673-2017, 2017.
- 702 Dulac, F., P. Buat-Ménard, M. Arnold, U. Ezat, and D. Martin, Atmospheric input of trace metals to the  
703 western Mediterranean Sea: 1. Factors controlling the variability of atmospheric concentrations, *J.*  
704 *Geophys. Res.*, 92(D7), 8437–8453, doi: 10.1029/JD092iD07p08437, 1987.
- 705 Evan, A.T., Flamant, C., Gaetani, M. et al.: The past, present and future of African dust, *Nature*, 531,  
706 493, 2016.
- 707 Formenti, P., Rajot, J. L., Desboeufs, K., Caquineau, S., Chevaillier, S., Nava, S., Gaudichet, A., Journet,  
708 E., Triquet, S., Alfaro, S., Chiari, M., Haywood, J., Coe, H., and Highwood, E.: Regional variability of the  
709 composition of mineral dust from western Africa: Results from the AMMA SOP0/DABEX and DODO  
710 field campaigns, *J. Geophys. Res.-Atmos.*, 113, *D00C13*, doi:10.1029/2008JD009903, 2008.
- 711 Formenti, P., Schütz, L., Balkanski, Y., Desboeufs, K., Ebert, M., Kandler, K., Petzold, A., Scheuven, D.,  
712 Weinbruch, S., and Zhang, D.: Recent progress in understanding physical and chemical properties of  
713 African and Asian mineral dust, *Atmos. Chem. Phys.*, 11, 8231-8256, 10.5194/acp-11-8231-2011,  
714 2011.
- 715 Formenti, P., Caquineau, S., Desboeufs, K., Klaver, A., Chevaillier, S., Journet, E., and Rajot, J. L.:  
716 Mapping the physico-chemical properties of mineral dust in western Africa: mineralogical  
717 composition, *Atmos. Chem. Phys.*, 14, 10663-10686, doi:10.5194/acp-14-10663-2014, 2014.
- 718 Fu, Y., Desboeufs, K., Vincent, J., Bon Nguyen, E., Laurent, B., Losno, R., and Dulac, F.: Estimating  
719 chemical composition of atmospheric deposition fluxes from mineral insoluble particles deposition  
720 collected in the Western Mediterranean region, *Atmos. Meas. Tech.*, 10, 4389–4401,  
721 doi:10.5194/amt-10-4389-2017, 2017.

- 722 Gallisai, R., Peters, F., Volpe, G., Basart, S., and Baldasano, J. M.: Saharan Dust Deposition May Affect  
723 Phytoplankton Growth in the Mediterranean Sea at Ecological Time Scales, *PLoS ONE*, 9, e110762,  
724 doi:10.1371/journal.pone.0110762, 2014.
- 725 Gratz, L. E., Keeler, G. J., Morishita, M., Barres, J. A., and Dvonch, J. T.: Assessing the emission sources  
726 of atmospheric mercury in wet deposition across Illinois, *Sci. Total Environ.*, 448, 120-131,  
727 doi:10.1016/j.scitotenv.2012.11.011, 2013.
- 728 Guerzoni, S., Chester, R., Dulac, F., Herut, B., Loÿe-Pilot, M.-D., Measures, C., Migon, C., Molinaroli, E.,  
729 Moulin, C., and Rossini, P.: The role of atmospheric deposition in the biogeochemistry of the  
730 Mediterranean Sea, *Progr. Oceanog.*, 44, 147-190, doi:10.1016/S0079-6611(99)00024-5, 1999a.
- 731 Guerzoni, S., Molinaroli, E., Rossini, P., Rampazzo, G., Quarantotto, G., De Falco, G., and Cristini, S.:  
732 Role of desert aerosol in metal fluxes in the Mediterranean area, *Chemosphere*, 39, 229-246, 1999b.
- 733 Guieu, C., Chester, R., Nimmo, M., Martin, J.-M., Guerzoni, S., Nicolas, E., Mateu, J., and Keyse, S.:  
734 Atmospheric input of dissolved and particulate metals to the northwestern Mediterranean, *Deep Sea*  
735 *Res. II*, 44, 655-674, doi:10.1016/S0967-0645(97)88508-6, 1997.
- 736 Guieu, C., Loÿe-Pilot, M. D., Benyahya, L., and Dufour, A.: Spatial variability of atmospheric fluxes of  
737 metals (Al, Fe, Cd, Zn and Pb) and phosphorus over the whole Mediterranean from a one-year  
738 monitoring experiment: Biogeochemical implications, *Mar. Chem.*, 120, 164-178,  
739 doi:10.1016/j.marchem.2009.02.004, 2010.
- 740 Heimburger, A., Losno, R., Triquet, S., Dulac, F., and Mahowald, N. C. G.: Direct measurements of  
741 atmospheric iron, cobalt, and aluminum-derived dust deposition at Kerguelen Islands, *Global*  
742 *Biogeochem. Cycles*, 26, doi:10.1029/2012gb004301, 2012.
- 743 Herut B., and Krom, M.: Atmospheric Input of Nutrients and Dust to the SE Mediterranean. In: Guerzoni  
744 S., Chester R. (eds) *The Impact of Desert Dust Across the Mediterranean*. Environmental Science and  
745 Technology Library, vol 11. Springer, Dordrecht, 1996.
- 746 Hovmand, M. F., Kemp, K., Kystol, J., Johnsen, I., Riis-Nielsen, T., and Pacyna, J. M.: Atmospheric heavy  
747 metal deposition accumulated in rural forest soils of southern Scandinavia, *Environ. Poll.*, 155, 537-  
748 541, doi:10.1016/j.envpol.2008.01.047, 2008.
- 749 Keeler, G.J., Landis, M.S., Norris, G.A., Christianson, E.M., and Dvonch, J.T.: Sources of mercury wet  
750 deposition in Eastern Ohio, USA, *Environ. Sci. Technol.*, 40, 5874-5881, doi:10.1021/es060377q,  
751 2006.
- 752 Krom, M. D., Emeis, K. C., and Van Cappellen, P.: Why is the Eastern Mediterranean phosphorus  
753 limited?, *Prog. Oceanog.*, 85, 236-244, doi:10.1016/j.pocean.2010.03.003, 2010.
- 754 Lazzari, P., Solidoro, C., Salon, S., and Bolzon, G.: Spatial variability of phosphate and nitrate in the  
755 Mediterranean Sea: A modeling approach, *Deep Sea Res. I*, 108, 39-52,  
756 doi:10.1016/j.dsr.2015.12.006, 2016.
- 757 Loÿe-Pilot, M. D., and Martin, J. M.: Saharan Dust Input to the Western Mediterranean: An Eleven Years  
758 Record in Corsica, in: *The Impact of Desert Dust Across the Mediterranean*, edited by: Guerzoni, S.,  
759 and Chester, R., Kluwer, 191-199, 1996.
- 760 Loÿe-Pilot, M.D., Guieu, C., Ridame, C., Atmospheric bulk fluxes of natural and pollutant metals to the  
761 north western Mediterranean; their trend over the past 15 years (1985–2000). *Atmospheric*  
762 *Transport and Deposition of Pollutants into the Mediterranean Sea —Final Reports on Research*  
763 *Project*. UNEP/MAP, Athens, pp. 35–54. MAP Technical Reports Series, 133, 2001.
- 764 Loÿe-Pilot, M.D., Martin, J.M. & Morelli, J.: Atmospheric input of inorganic nitrogen to the Western  
765 Mediterranean, *Biogeochem.*, 9, 117-134, doi:10.1007/BF00692168, 1990.

- 766 Mahowald, N., Jickells, T. D., Baker, A. R., Artaxo, P., Benitez-Nelson, C. R., Bergametti, G., Bond, T. C.,  
 767 Chen, Y., Cohen, D. D., Herut, B., Kubilay, N., Losno, R., Luo, C., Maenhaut, W., McGee, K. A., Okin, G.  
 768 S., Siefert, R. L., and Tsukuda, S.: Global distribution of atmospheric phosphorus sources,  
 769 concentrations and deposition rates, and anthropogenic impacts, *Global Biogeochem. Cycles*, 22,  
 770 doi:10.1029/2008gb003240, 2008.
- 771 Markaki, Z., Loýe-Pilot, M. D., Violaki, K., Benyahya, L., and Mihalopoulos, N.: Variability of atmospheric  
 772 deposition of dissolved nitrogen and phosphorus in the Mediterranean and possible link to the  
 773 anomalous seawater N/P ratio, *Mar. Chem.*, 120, 187-194, doi:10.1016/j.marchem.2008.10.005,  
 774 2010.
- 775 Mason, B., and Moore, C.B.: *Principles of Geochemistry*, 1982.
- 776 Morabito, E., Contini, D., Belosi, F., Stortini, A. M., Manodori, L., and Gambaro, A.: Atmospheric  
 777 Deposition of Inorganic Elements and Organic Compounds at the Inlets of the Venice Lagoon, *Adv.*  
 778 *Meteor.*, 2014, 10, doi:10.1155/2014/158902, 2014.
- 779 Morales-Baquero, R., Pulido-Villena, E., and Reche, I.: Chemical signature of Saharan dust on dry and  
 780 wet atmospheric deposition in the south-western Mediterranean region, *Tellus B*, 65,  
 781 10.3402/tellusb.v65i0.18720, 2013.
- 782 Morel, F. M. M., and Price, N. M.: The Biogeochemical Cycles of Trace Metals in the Oceans, *Science*,  
 783 300, 944-947, doi:10.1126/science.1083545, 2003.
- 784 Moulin, C., Lambert, C. E., Dulac, F., and Dayan, U.: Control of atmospheric export of dust from North  
 785 Africa by the North Atlantic Oscillation, *Nature*, 387, 691-694, doi:10.1038/42679, 1997.
- 786 Nava, S., Lucarelli, F., Amato, F., Becagli, S., Calzolari, G., Chiari, M., Giannoni, M., Traversi, R., and Udisti,  
 787 R.: Biomass burning contributions estimated by synergistic coupling of daily and hourly aerosol  
 788 composition records, *Sci. Tot. Environ.*, 511, 11–20, doi:10.1016/j.scitotenv.2014.11.034, 2015.
- 789 Norris, G., Duvall, R., and Brown, S.: *EPA Positive Matrix Factorization (PMF) 5.0 Fundamentals & User*  
 790 *Guide*, EPA, U.S., 2014.
- 791 O'Dowd, C. D. and Smith, M. H.: Physicochemical properties of aerosols over the northeast Atlantic:  
 792 Evidence for wind-speed related submicron sea-salt aerosol production, *J. Geophys. Res.*, 98, 1137–  
 793 1149, doi:10.1029/92JD02302, 1993.
- 794 Ochoa-Hueso, R., Allen, E. B., Branquinho, C., Cruz, C., Dias, T., Fenn, M. E., Manrique, E., Perez-Corona,  
 795 M. E., Sheppard, L. J., and Stock, W. D.: Nitrogen deposition effects on Mediterranean-type  
 796 ecosystems: An ecological assessment, *Environ. Poll.*, 159, 2265-2279,  
 797 doi:10.1016/j.envpol.2010.12.019, 2011.
- 798 Paatero, P., and Tapper, U.: Positive matrix factorization — a non-negative factor model with optimal  
 799 utilization of error-estimates of data values, *Environmetrics*, 5, 111–126,  
 800 doi:10.1002/env.3170050203, 1994.
- 801 Paatero, P. : Least squares formulation of robust non-negative factor analysis, *Chemom. Intell. Lab.*  
 802 *Syst.*, 37, 23-35, 1997.
- 803 Pey, J., Querol, X., and Alastuey, A.: Variations of levels and composition of PM10 and PM2.5 at an  
 804 insular site in the Western Mediterranean, *Atmos. Res.*, 94, 285–299,  
 805 doi:10.1016/j.atmosres.2009.06.006, 2009.
- 806 Polissar, A.V., Hopke, P.K., Poirot, R.L.: Atmospheric aerosol over Vermont: chemical composition and  
 807 sources, *Environ Sci Technol*, 35, 4604-4621, doi:10.1021/es0105865, 2001.
- 808 Pulido-Villena, E., Rérolle, V., and Guieu, C.: Transient fertilizing effect of dust in P-deficient LNL  
 809 surface ocean, *Geophys. Res. Lett.*, 37, L01603, doi:10.1029/2009gl041415, 2010.

810 Remoudaki, E., Bergametti, G., and Losno, R.: On the dynamic of the atmospheric input of copper and  
811 manganese into the Western Mediterranean Sea, *Atmos. Environ.*, 25A, 733-744, doi:10.1016/0960-  
812 1686(91)90072-F, 1991.

813 Ribera d'Alcalà, M., Civitarese, G., Conversano, F., and Lavezza, R. C.: Nutrient ratios and fluxes hint at  
814 overlooked processes in the Mediterranean Sea, *J. Geophys. Res. - Oceans*, 108,  
815 10.1029/2002jc001650, 2003.

816 Richon, C., Dutay, J.-C., Dulac, F., Wang, R., Balkanski, Y., Nabat, P., Aumont, O., Desboeufs, K., Laurent,  
817 B., Guieu, C., Raimbault, P., and Beuvier, J.: Modeling the impacts of atmospheric deposition of  
818 nitrogen and desert dust-derived phosphorus on nutrients and biological budgets of the  
819 Mediterranean Sea, *Prog. Oceanog.* doi:10.1016/j.pocean.2017.04.009, 2018a.

820 Richon, C., Dutay, J.-C., Dulac, F., Wang, R., and Balkanski, Y.: Modeling the biogeochemical impact of  
821 atmospheric phosphate deposition from desert dust and combustion sources to the Mediterranean  
822 Sea, *Biogeosciences*, 15, 2499-2524, <https://doi.org/10.5194/bg-15-2499-2018>, 2018b.

823 Ridame, C., Guieu, C., and Löye-Pilot, M. D.: Trend in total atmospheric deposition fluxes of aluminium,  
824 iron, and trace metals in the northwestern Mediterranean over the past decade (1985-1997), *J.*  
825 *Geophys. Res.*, 104, 30127-30138, doi:10.1029/1999JD900747, 1999.

826 Ridame, C., Le Moal, M., Guieu, C., TERNON, E., Biegala, I. C., L'Helguen, S., and Pujo-Pay, M.: Nutrient  
827 control of N<sub>2</sub> fixation in the oligotrophic Mediterranean Sea and the impact of Saharan dust events,  
828 *Biogeosci.*, 8, 2773-2783, doi:10.5194/bg-8-2773-2011, 2011.

829 Salvador, P., Alonso-Pérez, S., Pey, J., Artinano, B., de Bustos, J. J., Alastuey, A., and Querol, X.: African  
830 dust outbreaks over the western Mediterranean Basin: 11-year characterization of atmospheric  
831 circulation patterns and dust source areas, *Atmos. Chem. Phys.*, 14, 6759-6775, doi:10.5194/acp-14-  
832 6759-2014, 2014.

833 Sciare, J., Oikonomou, K., Favez, O., Liakakou, E., Markaki, Z., Cachier, H., and Mihalopoulos, N.: Long-  
834 term measurements of carbonaceous aerosols in the Eastern Mediterranean: evidence of long-range  
835 transport of biomass burning, *Atmos. Chem. Phys.*, 8, 5551-5563, doi:10.5194/acp-8-5551-2008,  
836 2008.

837 Sellegri, K., Gourdeau, J., Putaud, J.-P., and Despiou, S.: Chemical composition of marine aerosol in a  
838 Mediterranean coastal zone during the FETCH experiment, *J. Geophys. Res.*, 106, 12023,  
839 doi:10.1029/2000JD900629, 2001.

840 Tanaka, T., Thingstad, T. F., Christaki, U., Colombet, J., Cornet-Barthaux, V., Courties, C., Grattepanche,  
841 J. D., Lagaria, A., Nedoma, J., Oriol, L., Psarra, S., Pujo-Pay, M., and Van Wambeke, F.: Lack of P-  
842 limitation of phytoplankton and heterotrophic prokaryotes in surface waters of three anticyclonic  
843 eddies in the stratified Mediterranean Sea, *Biogeosci.*, 8, 525-538, doi:10.5194/bg-8-525-2011, 2011.

844 Tovar-Sánchez, A., Duarte, C. M., Arrieta, J. M., and Sañudo-Wilhelmy, S.: Spatial gradients in trace  
845 metal concentrations in the surface microlayer of the Mediterranean Sea, *Frontiers Mar. Sci.*, 1,  
846 doi:10.3389/fmars.2014.00079, 2014.

847 Vincent, J., Laurent, B., Losno, R., Bon Nguyen, E., Rouillet, P., Sauvage, S., Chevaillier, S., Coddeville, P.,  
848 Ouboulmane, N., di Sarra, A. G., Tovar-Sanchez, A., Sferlazzo, D., Massanet, A., Triquet, S., Morales  
849 Baquero, R., Fournier, M., Coursier, C., Desboeufs, K., Dulac, F., and Bergametti, G.: Variability of  
850 mineral dust deposition in the western Mediterranean basin and south-east of France, *Atmos. Chem.*  
851 *Phys.*, 16, 8749-8766, doi:10.5194/acp-16-8749-2016, 2016.

852 Violaki, K., Sciare, J., Williams, J., Baker, A. R., Martino, M., and Mihalopoulos, N.: Atmospheric water-  
853 soluble organic nitrogen (WSO<sub>N</sub>) over marine environments: a global perspective, *Biogeosci.*, 12,  
854 3131-3140, doi:10.5194/bg-12-3131-2015, 2015.

- 855 Violaki K., Bourrin F., Aubert D., Kouvarakis G., Delsaut N., Mihalopoulos N. Organic phosphorus in  
856 atmospheric deposition over the Mediterranean Sea: An important missing piece of the phosphorus  
857 cycle. Special issue of MERMEX project: Recent advances in the oceanography of the Mediterranean  
858 Sea, *Progress in Oceanography*, 163, 50-58, 2018.
- 859 Wai, K.-M., Wu, S., Li, X., Jaffe, D. A., and Perry, K. D.: Global Atmospheric Transport and Source-  
860 Receptor Relationships for Arsenic, *Environ. Sci. Technol.*, 50, 3714-3720,  
861 doi:10.1021/acs.est.5b05549, 2016.
- 862 Waldner, P., Marchetto, A., Thimonier, A., Schmitt, M., Rogora, M., Granke, O., Mues, V., Hansen, K.,  
863 Pihl Karlsson, G., Zlindra, D. et al.: Detection of temporal trends in atmospheric deposition of  
864 inorganic nitrogen and sulphate to forests in Europe, *Atmos. Environ.*, 95, 363-374,  
865 <https://doi.org/10.1016/j.atmosenv.2014.06.054>, 2014.
- 866